

**Degradation of Azo Dyes under Visible Light with Stable MOF
Based on Tetrastyrene Imidazole Ligand†**

Xiao Zhang^a, Lu-Jie Wang^a, Zhen Han^a, Xing Meng^a, Hai-Ning Wang^a, Zi-Yan Zhou^{a*} and Zhong-Min Su^{b,c*}

a. College of Chemistry and Chemical Engineering, Shandong University of Technology, Zibo, Shandong, 255049, People's Republic of China

b. School of Chemistry and Environmental Engineering, Changchun University of Science and Technology, Changchun, 130022, China

c. Jilin Provincial Science and Technology Innovation Center of Optical Materials and Chemistry, Changchun, 130022, China

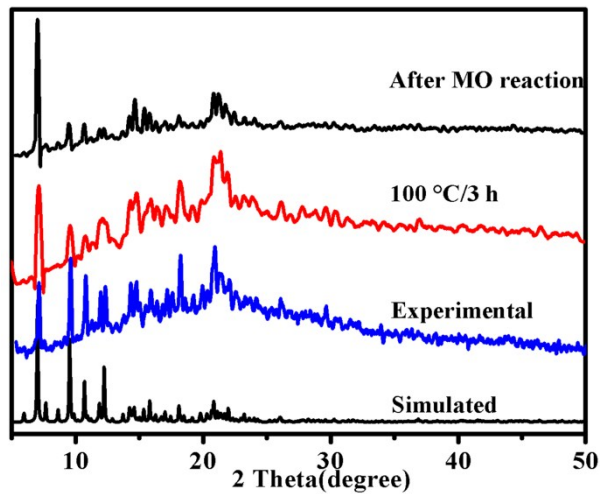


Fig. S1 PXRD of MOF before and after reaction and heated in boiling water for 3 h

It is found that the peak can be basically aligned, but the strength has some changes, because after degradation, some dye molecules adsorb on the crystal, resulting in the decrease of crystallinity of the crystal.

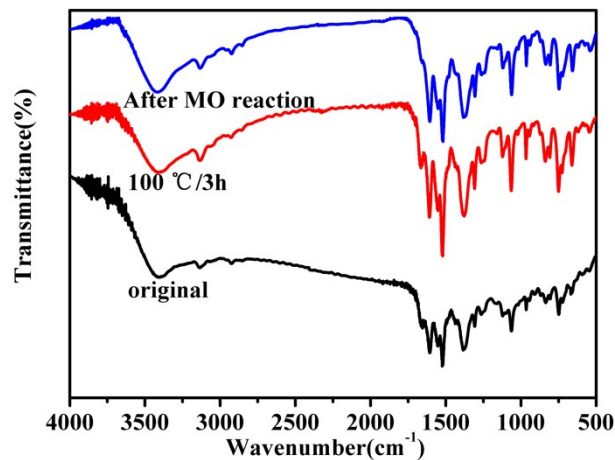


Fig. S2 FT-IR of MOF before and after reaction and heated in boiling water for 3 h

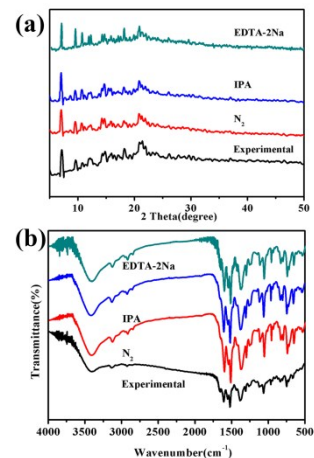


Fig. S3 PXRD and FT-IR of MOF before and after reaction with sacrificial agent

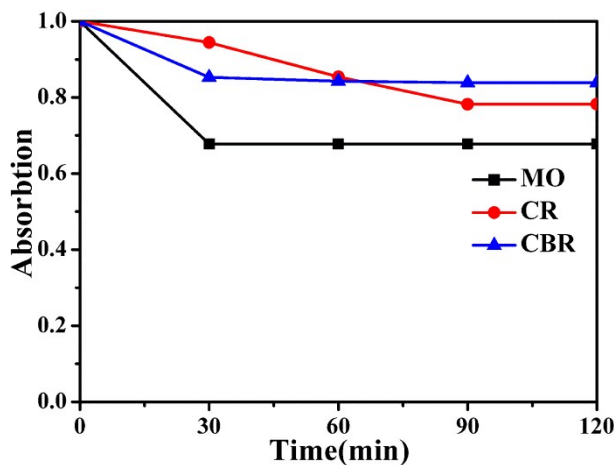


Fig. S4 Dark adsorption of all dyes at 293.15 K

Table S1 Design of 3-factor and 3-level orthogonal test of MO

Levels	Factors		
	pH (A)	MOFs/mg (B)	Initial MO/ 10^{-5} (mol/L) (C)
1	2.9	10	1
2	6.8	20	2
3	10.9	30	3

Table S2 Orthogonal experimental results of MO

Entry	pH (A)	MOFs/mg (B)	Initial MO/ 10^{-5} (mol/L) (C)	150min Degradation/%
1	1(2.9)	1(10)	1(1)	36.93
2	1(2.9)	2(20)	2(2)	87.27
3	1(2.9)	3(30)	3(3)	83.43
4	2(6.8)	1(10)	2(2)	96.48
5	2(6.8)	2(20)	3(3)	91.88
6	2(6.8)	3(30)	1(1)	77.66
7	3(10.9)	1(10)	3(3)	37.99
8	3(10.9)	2(20)	1(1)	60.85
9	3(10.9)	3(30)	2(2)	74.65

Table S3 Optimization results of MO

Entry	pH (A)	MOFs/mg (B)	Initial MO/ 10^{-5} (mol/L) (C)
K1	207.63	171.40	175.44
K2	266.02	240.00	258.40
K3	173.49	235.74	213.30

\bar{K}_1	69.21	57.13	58.48
\bar{K}_2	88.67	80.00	86.13
\bar{K}_3	57.83	78.58	71.10
R	30.84	22.87	27.65

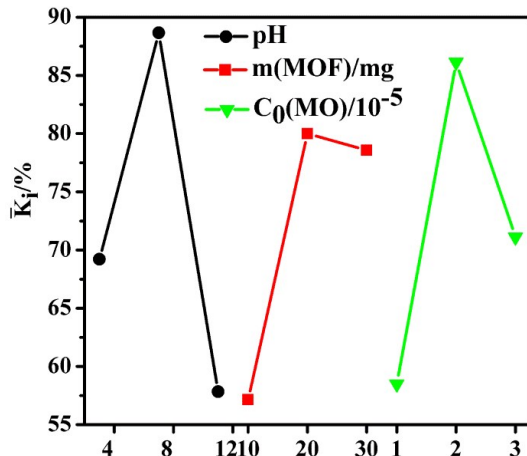


Fig. S5 \bar{K}_i vs the levels of the factors for MO

Table S4 Design of 3-factor and 3-level orthogonal test of CR

Levels	Factors		
	pH (A)	MOFs/mg (B)	Initial CR/ 10^{-5} (mol/L) (C)
1	2.9	10	1
2	6.8	15	2
3	10.9	20	3

Table S5 Orthogonal experimental results of CR

Entry	pH (A)	MOFs/mg (B)	Initial CR/ 10^{-5} (mol/L) (C)	250min Degradation/%
1	1(2.9)	1(10)	1(1)	50.76
2	1(2.9)	2(15)	2(2)	43.74
3	1(2.9)	3(20)	3(3)	46.57
4	2(6.8)	1(10)	2(2)	40.81
5	2(6.8)	2(15)	3(3)	42.87
6	2(6.8)	3(20)	1(1)	38.46
7	3(10.9)	1(10)	3(3)	44.37
8	3(10.9)	2(15)	1(1)	35.16
9	3(10.9)	3(20)	2(2)	38.63

Table S6 Optimization results of CR

Entry	pH (A)	MOFs/mg (B)	Initial CR/ 10^{-5} (mol/L) (C)
K1	141.07	135.94	124.38
K2	122.14	121.77	123.18

K3	118.16	123.66	133.81
\bar{K}_1	47.02	45.31	41.46
\bar{K}_2	40.71	40.59	41.06
\bar{K}_3	39.39	41.22	44.60
R	8.32	4.72	3.54

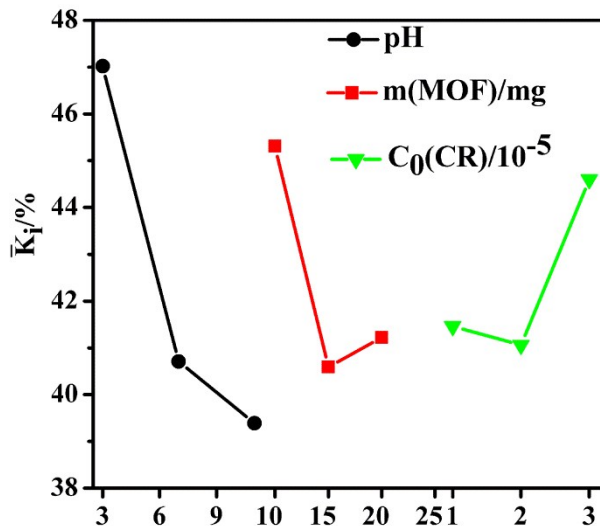


Fig. S6 \bar{K}_1 vs the levels of the factors for CR

Table S7 Design of 3-factor and 3-level orthogonal test of CBR

Levels	Factors		
	pH (A)	MOFs/mg (B)	Initial CBR/10⁻⁵(mol/L) (C)
1	2.9	10	1
2	6.8	20	2
3	10.9	30	3

Table S8 Orthogonal experimental results of CBR

Entry	pH (A)	MOFs/mg (B)	Initial CBR/10⁻⁵(mol/L) (C)	300min Degradation/%
1	1(2.9)	1(10)	1(1)	84.15
2	1(2.9)	2(20)	2(2)	77.74
3	1(2.9)	3(30)	3(3)	75.69
4	2(6.8)	1(10)	2(2)	89.63
5	2(6.8)	2(20)	3(3)	83.54
6	2(6.8)	3(30)	1(1)	90.73
7	3(10.9)	1(10)	3(3)	79.48
8	3(10.9)	2(20)	1(1)	83.75
9	3(10.9)	3(30)	2(2)	76.92

Table S9 Optimization results of CBR

Entry	pH	MOFs/mg	Initial CBR/10⁻⁵(mol/L)
-------	----	---------	-------------------------

	(A)	(B)	(C)
K1	237.58	253.26	258.63
K2	263.90	245.03	244.29
K3	240.15	243.34	238.71
\bar{K}_1	79.19	84.42	86.21
\bar{K}_2	87.97	81.68	81.43
\bar{K}_3	80.05	81.11	79.57
R	8.78	3.31	6.64

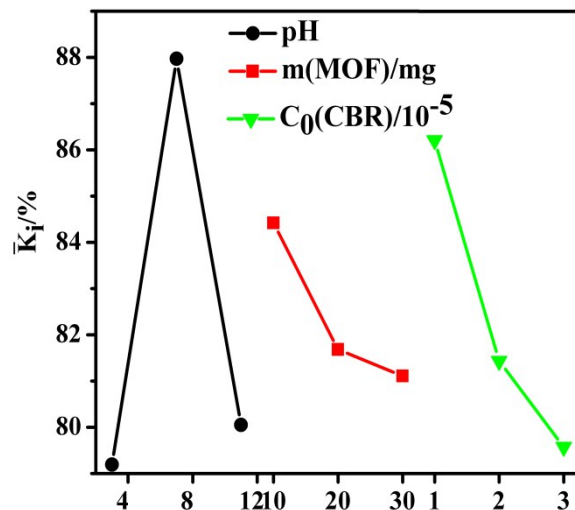


Fig. S7 \bar{K}_1 vs the levels of the factors for CBR

Table S10 The reaction rate constants of degrade dyes in different temperature

Dye	Temperature(K)	$K_f (\text{min}^{-1})$	R^2	$Ea(\text{kJ/mol})$	$R^2 \text{ of } E_a$
MO	293.15	0.0110	0.9942	23.49	0.9941
	303.15	0.0149	0.9910		
	308.15	0.0170	0.9919		
	313.15	0.0199	0.9927		
	318.15	0.0238	0.9936		
	293.15	0.0033	0.9871		
CR	303.15	0.0060	0.9810	52.68	0.9851
	308.15	0.0098	0.9959		
	313.15	0.0142	0.9958		
	318.15	0.0170	0.9887		
CBR	293.15	0.0097	0.9967	15.19	0.9932
	303.15	0.0115	0.9974		
	308.15	0.0126	0.9984		
	313.15	0.0146	0.9978		

318.15

0.0169

0.9953

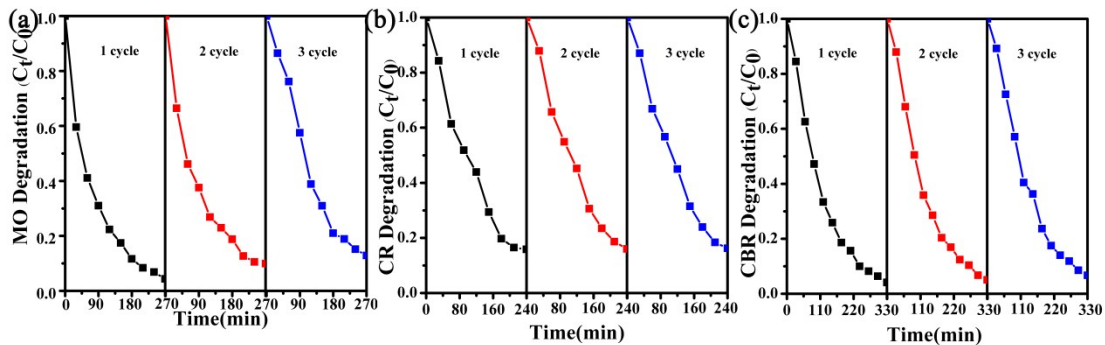


Fig. S8 Cycling runs for the photocatalytic degradation of MO (a), CR (b), CBR (c), over catalyst **MOF** under visible light irradiation. (Reaction conditions: $[MO] = 2.0 \times 10^{-5}$ M, pH = 6.8, $[MOF] = 20$ mg, T = 293.15 K; $[CR] = 3.0 \times 10^{-5}$ M, pH = 2.9, $[MOF] = 10$ mg, T = 293.15 K; $[CBR] = 1.0 \times 10^{-5}$ M, pH = 6.8, $[MOF] = 10$ mg, T = 293.15 K.

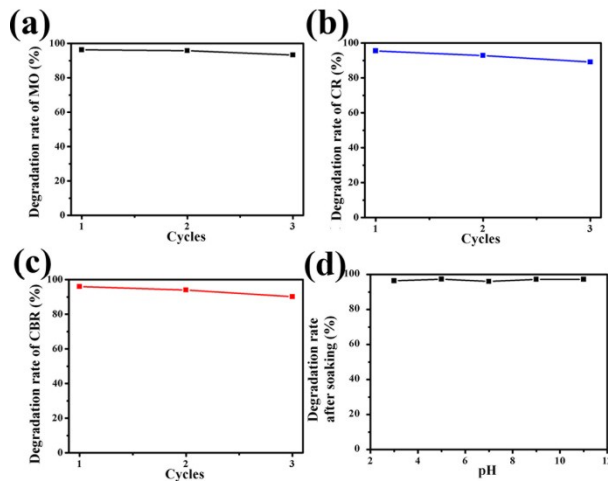


Fig. S9 Cycling runs for the photocatalytic degradation rate of MO (a), CR (b), CBR (c), over catalyst 1 under natural light irradiation at room temperature. (d) The degradation rate after soaking (Reaction conditions: $[MO] = 2.0 \times 10^{-5}$ M, pH = 6.8, $[MOF] = 20$ mg, T = 293.15 K; $[CR] = 3.0 \times 10^{-5}$ M, pH = 2.9, $[MOF] = 10$ mg, T = 293.15 K; $[CBR] = 1.0 \times 10^{-5}$ M, pH = 6.8, $[MOF] = 10$ mg, T = 293.15 K).

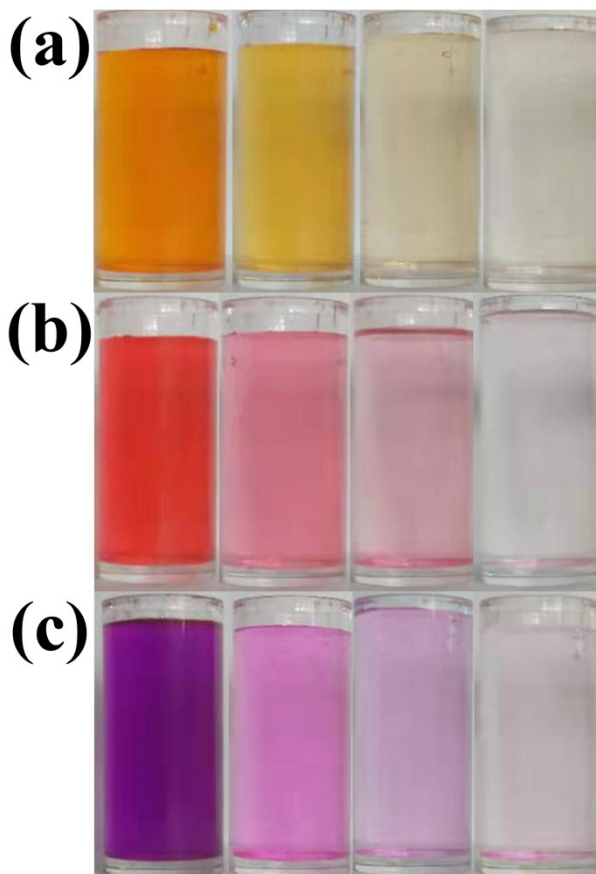


Fig. S10 Dye solutions after different degradation times under optimal conditions.(Reaction conditions: $[MO] = 2.0 \times 10^{-5}$ M, pH = 6.8, [MOF] = 20 mg, T = 293.15 K; [CR] = 3.0×10^{-5} M, pH = 2.9, [MOF] = 10 mg, T = 293.15 K; [CBR] = 1.0×10^{-5} M, pH = 6.8, [MOF] = 10 mg, T = 293.15 K)

X-ray Crystallographic Study^[1-2]

Single-crystal X-ray diffraction data recorded on a Bruker Smart Apex II CCD diffractometer with graphite-monochromated Mo K α radiation ($\lambda = 0.71073$ Å) by the ω and θ scan mode at room temperature. The structure was solved by the direct method and refined by the full matrix least-squares method on F² using the SHELXTL 2014 crystallographic software package. Crystallographic data for the structures reported in this paper have been deposited in the Cambridge Crystallographic Data Center with CCDC reference number 1909962 for MOF.

References

1. G. M. Sheldrick, *Acta Crystallogr. C*, 2015, **71**, 3-8.
2. Isabel Usón and G. M. Sheldrick, *Acta Crystallogr. D*, 2018, **74**, 106-116.